SHAKING TABLE TEST OF THE RC PARTLY-FRAMED SHEAR WALL STRUCTURE WITH CONCEALED BRACINGS

ZHANG Jianwei[1] , CAO Wanlin[1], HUANG Xuanming[2] and WANG Min[1]

[1]*College of Architecture and Civil Engineering, Beijing University of Technology, Beijing   China*
[2]*Academy of Building Research, Beijing, China*
Email: zhangjw@bjut.edu.cn

ABSTRACT:
Two models of RC shear wall structures with and without concealed bracings were tested on a shaking table, and the results are reported here. The test procedures took the structure through elastic, cracking and failure stages. Dynamic characteristics and responses of the structures at different stages were studied, and a comparison of failure modes between   two models is also made. Results from the tests indicate that before concrete cracking, seismic performance of a shear wall structure with concealed bracings is similar to that without concealed bracings. After concrete cracking, the resistance of the former to earthquake excitation is much better than that of the latter, the displacement response of the former is much smaller than that of the latter on the ground floor, and the cracks distributing height of the shear wall with concealed bracings is higher than that of the shear wall without concealed bracings.
KEY WORDS: reinforced concrete, shear wall structure, concealed bracing, shaking table test

1. INTRODUCTION

In order to improve the ductility of shear walls, RC shear walls with concealed bracings have been proposed by Cao (1998). Experiments have been conducted on many kinds of low-rise and mid-rise shear walls under low-frequency cyclic loading since 1999 (Cao *et al.* 1999, Dong *et al.* 2001, 2002 and Cao *et al.* 2003). The results from those experiments showed that the seismic performance of low-rise and mid-rise shear walls can be significantly improved by adding concealed bracings within the wall structures, and it is found that not only the load-carrying capacity and ductility are improved significantly, but also the structural performance can be stabilized significantly. In order to evaluate the performance of high-rise shear wall structures with concealed bracings subjected to dynamic loading, two partly-framed shear wall structures were designed according to the actual application of shear walls with concealed bracings in engineering construction practice. Shaking table tests were carried out and a comparison of seismic performance was made between the shear wall structure with concealed bracings and the normal shear wall structure without concealed bracings. The test results indicate that the application of concealed bracings enhances the shear wall load-carrying capacity greatly. In addition, the plastic hinge areas at the foot of the structure evidently deform, and the ductility was also improved significantly.
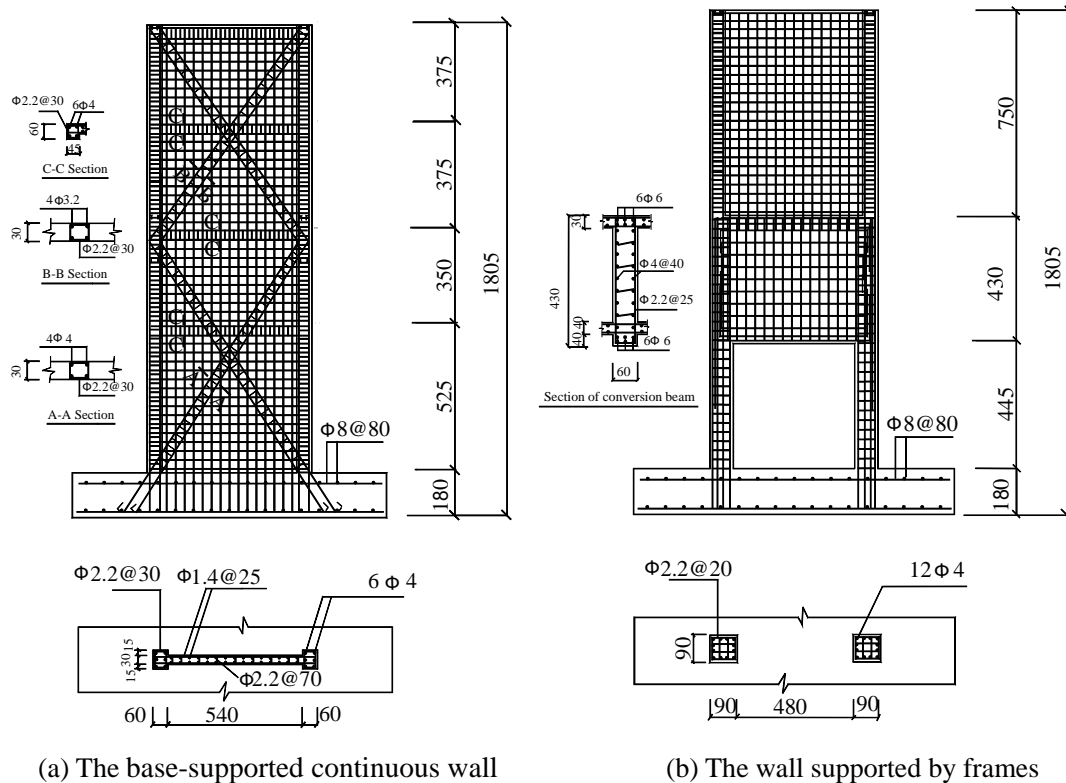
2. EXPERIMENTAL DETAILS

Considering the capacity of the shaking table to be used, two 1:8 scale shear wall structural models supported

partly by frames with large space on the ground floor were constructed. Each shear wall structure consisted of two base-supported continuous walls on both sides and a wall supported by frames in the middle of the structure.

The walls of each model were connected by floor slabs and coupling wall-beams, and the two models had the same dimensions. As shown in Figure 1, the models had four stories and large space on the ground floor.

The heights of the model's first story and the second story were 525 mm and 350 mm, respectively; the second story is the transfer story. The third and the fourth are the standard stories and their heights were both 375 mm. The axis distance between the base-supported continuous walls was 2100 mm for the both models. The test models are labeled as SW and SBW. SW represents the

Figure 1 Model fixed on shaking table

normal shear wall structure and SBW represents the shear wall structure with concealed bracings; the latter had concealed bracings in the base-supported continuous walls on both sides. The dimensions and reinforcement details of the base-supported continuous walls for the SBW model are illustrated in Figure 2(a), where the ratio of height to width is 2.46 and the weight ratio of concealed bracings reinforcement to total reinforcement is 0.24 for the base-supported continuous walls. The dimensions and reinforcement details for the walls supported by frames are illustrated in Figure 2(b). The dimensions and reinforcement details of SW and SBW walls were identical except no concealed bracings reinforcements employed for SW walls. The equivalent shear stiffness ratio of the third story to the first story is 2.0 (JGJ3—2002).

(a) The base-supported continuous wall (b) The wall supported by frames

Figure 2 Dimensions and reinforcement details for SBW model

The two models were cast with fine-aggregate concrete, which was designed with strength grade C30, and the mix proportion of concrete was 1: 1.20: 2.68: 0.48 (cement: sand: carpolite: water). The measured cube

compressive strength of concrete was 40.2 MPa, and the elastic modulus was 2.76×10^4 MPa. The ø6, ø4 steel bars and from 12[#] to 16[#] steel wires used in the models had the mechanical properties shown in Table 1.

In order to conform to the similitude requirements of mass and living loads, a total of 6.04 tons of steel blocks were fixed on the floors for each model. 1.09 tons of the total were attached to the first floor and the remaining masses were applied to other stories with 1.65 tons per floor. The dynamic similitude parameters of the model are as follows: dimension $C_l=1/8=0.125$, elastic modulus $C_E=1$, stress $C_\sigma=C_E=1$, mass density $C_\rho=C_\sigma/C_l=8$, mass $C_m=C_\rho C_l^3=0.016$, stiffness $C_k=C_E C_l=0.125$, time $C_t=(C_m/C_k)^{1/2}=0.354$, frequency $C_f=1/C_t=2.828$ and acceleration $C_a=C_l/C_t^2=1$.

Table 1 Mechanical Properties of Reinforcements

Diameter (mm)	Area (mm^2)	Yield Strength f_y(N/mm^2)	Ultimate Strength f_u(N/mm^2)	Elastic Modulus E_s(N/mm^2)
6	28.26	525	610	1.84×10^5
4	12.56	655	770	1.90×10^5
3.2	8.04	300	410	2.07×10^5
2.2	3.80	230	315	1.88×10^5
1.4	1.54	355	420	1.87×10^5

3 EXPERIMENTAL PROCESS AND RESULTS

3.1 Experiment Measurables

During the experimental sequence, measurements were taken of the following: (1) free vibration characteristics (natural frequencies, vibration modes, damping ratios), (2) lateral absolute acceleration responses at each story and at the surface of the shaking table, (3) lateral interstory drift, (4) strain of the main steel bars in the edge columns of the base-supported continuous walls, (5) strain of steel bars of the concealed bracings at the bottom and in the middle of the base-supported continuous walls, and (6) strain of the concrete at the bottom of the edge columns of the base-supported continuous walls. Details of these measurements are described below.

Table 2 Test procedure

SW Model			SBW Model		
No.	Degree	Input	No.	Degree	Input
1	7	0.069g	1	7	0.071g
2	7	0.134g	2	7	0.136g
3	7	0.231g	3	7	0.237g
4		0.307g	4		0.344g
5	8	0.428g	5	8	0.432g
6		0.501g	6		0.538g
7	9	0.622g	7	9	0.703g
8		0.823g	8		0.739g
9		0.928g	9		0.947g
10		1.04g	10		1.03g
11		1.17g	11		1.11g
12		1.18g	12		1.23g
			13		1.32g
			14		1.44g
			15		1.66g
			16		1.86g

3.2 Experimental Procedure

The two models were subjected to shaking table motions that simulated the El Centro (1940)N-S component earthquake ground motions, and the magnitude of peak ground acceleration(PGA) was varied over the approximate range of 0.05g, 0.1g, 0.2g, 0.3g et al. The actual PGA registered by the accelerometer on the surface of the shaking table during the experiment are shown in Table 2. The time scale was compressed by the factor of $\sqrt{1/8}=0.354$, according to the similitude law. The scaled values of time interval and duration of time

of the earthquake motions were then 0.02×0.354=0.00708s and 50×0.354=17.70s, respectively.

The free vibration tests for each model were made before and after concrete cracking. First, two accelerometers were fixed at the first story and the roof. Second, the model was excited by a sine wave motion produced by a signal generator which was set at the roof of the model. The signal generator was tuned to control the excitation wave frequency, with amplitude and phase of the waveform being shown at the oscillograph which was gathered from the additional accelerometers; frequency was varied until resonance occurred on one natural frequency of the model. The acceleration response of each story was gathered simultaneously. Third, the excitation was stopped and the decrement acceleration response of each story was gathered. Using the above data, the natural frequencies, vibration modes and damping ratios of the model were obtained by analyses of the acceleration response. The test program of free vibration characteristic is presented in Table 3; the different test times are numbered.

Table 3　Measured procedure of dynamic characteristic

SW Model		SBW Model	
No.	Test Time	No.	Test Time
1	Before earthquake excitation	1	Before earthquake excitation
2	After earthquake excitation with the PGA of 0.307g (cracking)	2	After earthquake excitation with the PGA of 0.703g (cracking)
3	After earthquake excitation with the PGA of 0.501g	3	After earthquake excitation with the PGA of 1.03g
4	After earthquake excitation with the PGA of 1.04g	4	After earthquake excitation with the PGA of 1.11g
5	After earthquake excitation with the PGA of 1.17g (Failure)	5	After earthquake excitation with the PGA of 1.32g
6		6	After earthquake excitation with the PGA of 1.66g (Failure)
7		7	After earthquake excitation with the PGA of 1.86g (Failure)

Table 4　Frequencies and damping ratios test results

SW Model					SBW Model				
No. of Test Time	First Natural Frequency (Hz)	First Damping Ratio	Second Natural Frequency (Hz)	Second Damping Ratio	No. of Test Time	First Natural Frequency (Hz)	First Damping Ratio	Second Natural Frequency (Hz)	Second Damping Ratio
1	17.53	0.01459	77.25	0.00766	1	17.59	0.01437	81.97	0.01108
2	16.23	0.01547	77.00	0.00833	2	15.94	0.01496	77.58	0.01109
3	15.15	0.01560	75.46	0.00879	3	13.28	0.01563	68.21	0.01129
4	11.52	0.02514	60.36	0.01104	4	12.71	0.01654	64.81	0.01188
5	11.25	0.02966	52.13	0.01277	5	11.75	0.01728	57.55	0.01240
					6	10.56	0.01778	47.45	0.01344
					7	9.56	0.02226	44.90	0.01545

3.3 Experiment Results and Interpretation

3.3.1 Natural Frequencies and Damping Ratios

The first two natural frequencies and damping ratios at different experimental stages are given in Table 4. In Table 4, noting the different test times, it can be seen that before concrete cracking, the natural frequencies and damping ratios of the two models are similar. After concrete cracking, the decrement of natural frequency for SBW is slower than that for SW while the increase of damping ratio for SBW is slower than that for SW. It is proposed that the bolt pin function of the concealed bracings stays and restricts the development of cracking, which slow down the stiffness degradation of SBW compared to SW.

3.3.2 Vibration Modes

The first two vibration modes of the models were measured during the experiment. A comparison of the first and second vibration modes, before and after concrete cracking, for SW and SBW are shown in Figures 3 and 4, respectively. The data indicate that the vibration modes of the two models are all flexure-shear patterns before concrete cracking. After concrete cracking, the ground floor of each model's vibration mode show a tendency to protrude. The vibration modes of SBW are similar to those of SW before concrete cracking; after concrete cracking, the ground floor of the first vibration mode for SW show a tendency to protrude before that for SBW while the second vibration mode of the two models are similar.
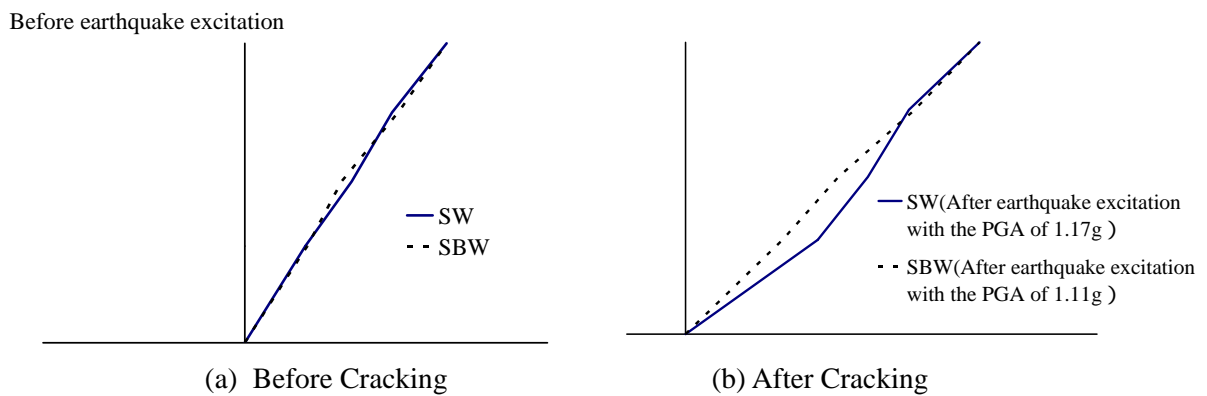

(a) Before Cracking   (b) After Cracking

Figure 3   First vibration mode

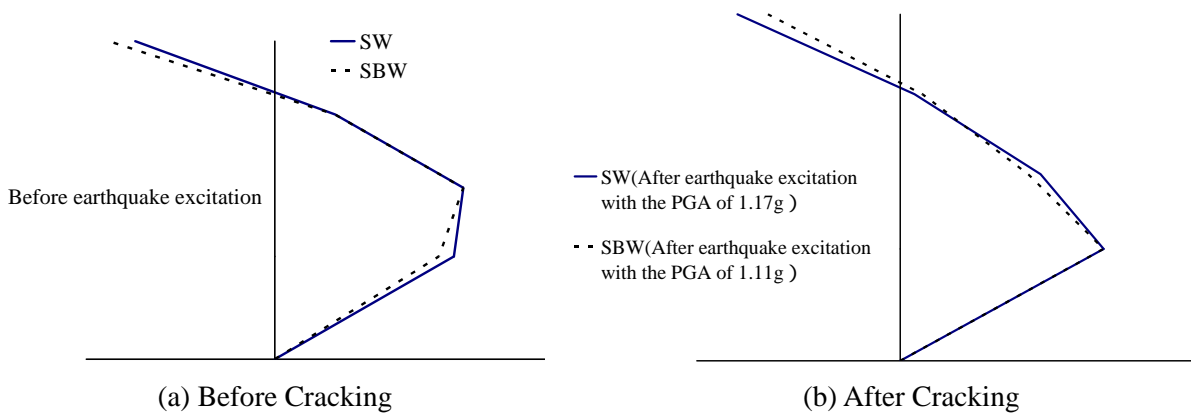

(a) Before Cracking   (b) After Cracking

Figure 4   Second vibration mode

3.3.3 Acceleration Response

The maximum values of the absolute accelerations for the two models are measured at each story and listed in Table 5. After concrete cracking, A comparison of the absolute accelerations of the roofs for SW and SBW is shown in Figure 5.

From Table 5 and Figure 5 several observations can be made. Before concrete cracking, the acceleration responses of the two models are similar undergone the same level of ground motion. The peak ground acceleration of SBW when the concrete cracks appear is increased by 129% compared with that undergone by SW, when the ultimate failure happens. Also, the peak ground acceleration undergone by SBW is increased by 57.63% compared with that undergone by SW.

Table 5   Maximum acceleration response of different floor

SW Model					SBW Model				
Input (g)	First Floor (g)	Second Floor (g)	Third Floor (g)	Fourth Floor (g)	Input (g)	First Floor (g)	Second Floor (g)	Third Floor (g)	Fourth Floor (g)
0.231	0.268	0.297	0.358	0.460	0.237	0.307	0.333	0.371	0.430
0.307	0.394	0.432	0.519	0.638	0.344	0.437	0.470	0.521	0.608
0.428	0.518	0.561	0.677	0.856	0.432	0.531	0.564	0.656	0.783
0.501	0.572	0.656	0.797	1.04	0.538	0.623	0.689	0.827	0.961
0.622	0.679	0.783	0.949	1.23	0.703	0.714	0.838	0.991	1.14
0.823	0.886	0.987	1.14	1.46	0.739	0.903	0.959	1.19	1.53
0.928	1.09	1.13	1.34	1.82	0.947	0.999	1.08	1.35	1.67
1.04	1.22	1.28	1.49	1.92	1.03	1.17	1.33	1.47	1.79
1.17	1.53	1.55	1.67	2.00	1.11	1.29	1.38	1.65	1.94
1.18	-----	-----	-----	-----	1.23	1.45	1.62	1.83	2.19
					1.32	1.52	1.73	2.04	2.40
					1.44	1.59	1.75	2.14	2.51
					1.66	1.74	1.80	2.19	2.70
					1.86	2.01	2.29	2.39	3.17

3.3.4 Interstory Drift Response

The maximum quantities of each interstory drift of the two models are listed in Table 6. Figure 6 illustrates the ground floor time histories for SBW and SW undergone the same level of ground motion.

It can be determined from Table 6 and Figure 6 that for the two models the interstory drift of the ground floor is significantly larger than that
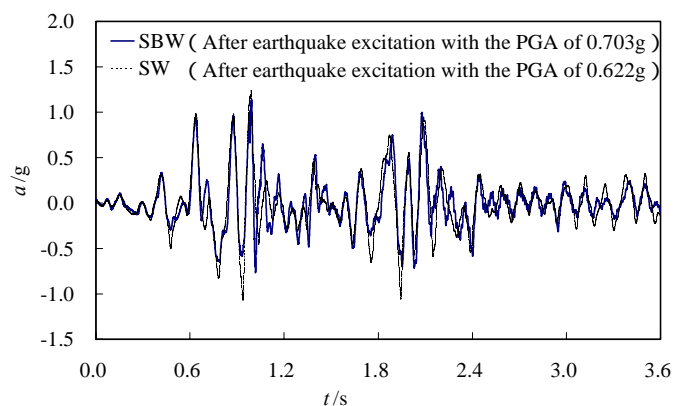

Figure 5   Acceleration response at top floor after cracking

of the other three stories. At the early stage, the interstory drift of each story for SW is similar with the corresponding story for SBW undergoing the same level of ground motion. After concrete cracking, the interstory drift of the ground floor for SBW is significantly less than that for SW.

Table 6   Maximum interstory drift response of different floor

SW Model					SBW Model				
Input (g)	First Floor (mm)	Second Floor (mm)	Third Floor (mm)	Fourth Floor (mm)	Input (g)	First Floor (mm)	Second Floor (mm)	Third Floor (mm)	Fourth Floor (mm)
0.231	0.038	0.014	0.014	0.018	0.237	0.026	0.017	0.014	0.013
0.307	0.063	0.018	0.019	0.020	0.344	0.037	0.025	0.020	0.021
0.428	0.087	0.026	0.023	0.028	0.432	0.051	0.031	0.021	0.026
0.501	0.133	0.029	0.023	0.036	0.538	0.057	0.032	0.024	0.030
0.622	0.309	0.047	0.033	0.043	0.703	0.115	0.055	0.047	0.041
0.823	0.566	0.057	0.039	0.051	0.739	0.259	0.067	0.048	0.048
0.928	0.859	0.083	0.047	0.069	0.947	0.471	0.072	0.050	0.061
1.04	1.22	0.097	0.060	0.077	1.03	0.640	0.099	0.066	0.068
1.17	1.61	0.148	0.109	0.093	1.11	0.895	0.122	0.097	0.093
1.18	2.10	----	----	----	1.23	1.18	0.118	0.069	0.081
					1.32	1.43	0.127	0.063	0.088
					1.44	1.69	0.125	0.063	0.086
					1.66	2.11	0.136	0.068	0.094
					1.86	2.99	0.204	0.127	0.159

3.3.5 Shearing Force Response of the Stories

Under the ground motions, the maximum nominal story shearing force of the number i story at the moment t (Li et $al.$ 2002), $F_i(t)_{max}$, can be determined by:

$$F_i(t)_{max} = \left| -\sum_{j=i}^{n} m_j a_j(t) \right|_{max} \qquad (1)$$

where n is the number of the stories, a_j is the acceleration of the number j story (j=1,2,3,4), m_j is the centralized mass of number j story. The

Figure 6 Interstory drift response at first floor after cracking

maximum values of the base shearing force are given in Table 7. It can be concluded from this table that the maximum nominal base shearing force endured by SBW is increased by 33.64% compared with SW.

3.3.6 Failure Modes

The following sequence of events occurred with the SW model. When the model was   subjected to earthquake
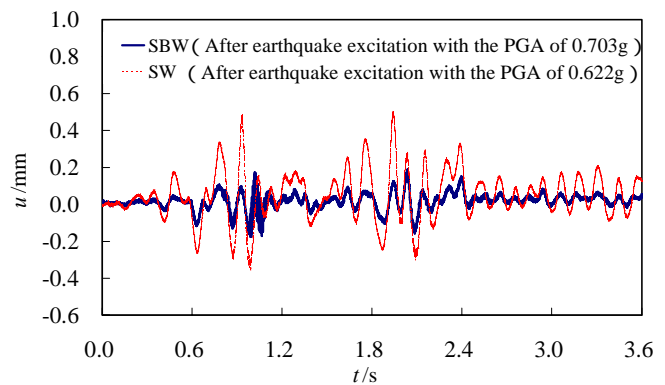
excitation with the peak ground acceleration of 0.307g (the fourth input), horizontal cracks began to appear at the bottom of the edge columns for the base-supported continuous walls. When the structure model was subjected to earthquake excitation with peak ground acceleration of 0.428g (the fifth input), the horizontal cracks on the edge columns developed toward the inside into a longer horizontal crack; this developed further as the experiment continued until the crack ran through the whole wall and developed into only one major crack. The concrete on crack locations began to fall off when the model was excited by the earthquake excitation with peak ground acceleration of 0.928g (the ninth input). After excitation with peak ground acceleration of 1.17g (the eleventh input), the concrete at the base of the edge columns for the base-supported continuous walls was crushed, and the vertical steel bars in the edge columns were pressed to flection; this indicated the failure of the walls. At the same time, cracks appeared at the middle and bottom of the columns supporting the shear wall. After earthquake excition with peak ground acceleration of 1.18g (the twelfth input), the base-supported continuous walls were severely damaged and a slide occured in the crack area. Meanwhile, new horizontal cracks developed at the middle bottom of the columns supporting the shear wall, but the columns did not reach failure.

The following sequence of events occurred for the SBW model. When it was subjected to earthquake excitation with peak ground acceleration of 0.703g (the seventh input), horizontal cracks, which almost run through the whole wall, began to occur at the bottom of the base-supported continuous walls , and the cracks continued to develop. After earthquake excitation with peak ground acceleration of 1.03g (the tenth input) long diagonal cracks, appeared at the middle sides of the ground floor walls which were supported by base, developed toward the middle and then ran through the wall. After earthquake excitation with peak ground acceleration of 1.11g (the eleventh input), the concrete on cracks began to fall off. After earthquake excitation with peak ground acceleration of 1.32g (the thirteenth input), horizontal cracks began to appear and new widespread horizontal cracks occurred at the middle bottom of the columns supporting the wall. After earthquake excitation with peak ground acceleration of 1.66g (the fifteenth input), the concrete at the base of the edge columns for the base-supported continuous walls was crushed and the vertical steel bars in the edge columns were pressed to flection; this indicated the failure of the walls. After earthquake excitation with peak ground acceleration of 1.86g (the sixteenth input), the walls were destroyed but slippage did not appear in the area of cracks; the columns did not reach failure.

The ultimate failure modes for the model walls are shown in Figure 7. From this figure and the failure mode

Table 7 Maximum shearing force on the top of basis

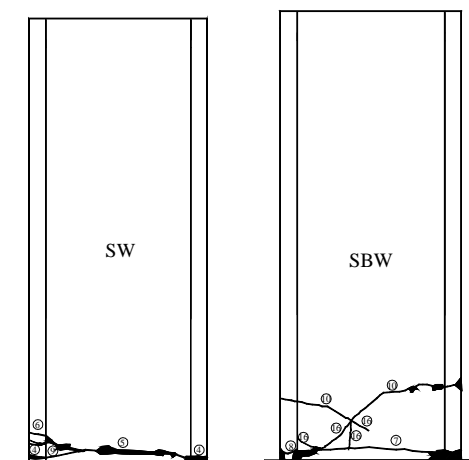| SW Model		SBW Model	
Input (g)	F *(kN)*	Input (g)	F (kN)
0.231	22.3	0.237	23.8
0.307	32.2	0.344	33.2
0.428	42.2	0.432	39.8
0.501	49.4	0.538	51.6
0.622	58.8	0.703	58.4
0.823	71.5	0.739	71.4
0.928	78.1	0.947	80.1
1.04	89.7	1.03	91.5
1.17	107	1.11	102
1.18	----	1.23	116
		1.32	129
		1.44	132
		1.66	136
		1.86	143

Figure 7 Failure mode for shear wall

depicted in the front, it can be seen that the walls were bent to failure, but the failure modes were different for the two models. For SW, only one main horizontal crack appeared at the bottom of the base-supported continuous walls; however, for SBW, the main cracks appeared at the bottom and the middle of the ground floor walls which were supported by base, which indicates that the height of the plastic hinge areas at the bottom of the walls with concealed bracings were significantly larger than that of the normal walls without concealed bracings. The proposed reason for this is that the concealed bracings enlarged the plastic hinge areas along with resisting the shearing force, and the enlargement builds up the capacity for energy dissipation. The design idea is similar to the equal strength beam designing idea. For the normal shear walls, horizontal slippage appeared at the bottom when the walls reached failure; while for the shear walls with concealed bracings, the bottom horizontal slippage did not appear as a result of the bolt pin function of the concealed bracings.

4 ANALYSIS OF EARTHQUAKE RESPONSE

4.1 Elastic Time History Analysis

Using SAP, finite element time history analyses were made for the two models. Rectangle plane elements with four nodes were used to simulate the shear walls and member elements were used to simulate the columns supporting the shear wall. The elastic modulus of the reinforced concrete was calculated using the following formula,

$$E = \rho_c E_c + \rho_s E_s \qquad\qquad 2$$

where ρ_c E_c are the volume ratio and the elastic modulus of the concrete, respectively, and ρ_s E_s are the volume ratio and the elastic modulus of the steel bar, respectively.

The calculation results for the first two natural frequencies are given in Table 8. The first two vibration modes are shown in Figure 8. The calculated and measured top floor absolute acceleration response for SW and SBW are plotted in Figures 9 and 10, respectively.

Table 8 Calculation and test results of frequency

Frequency	SW Model			SBW Model		
	Calculated (Hz)	Measured (Hz)	Percent Error (%)	Calculated (Hz)	Measured (Hz)	Percent Error (%)
First	18.69	17.53	6.62	18.87	17.59	7.28
Second	78.13	77.25	1.14	79.37	81.97	-3.17
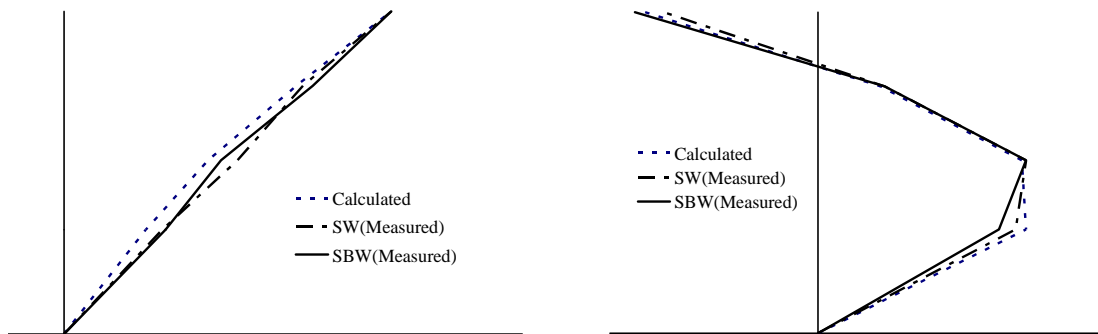
(a)　First vibration mode　　　　　(b) Second vibration mode

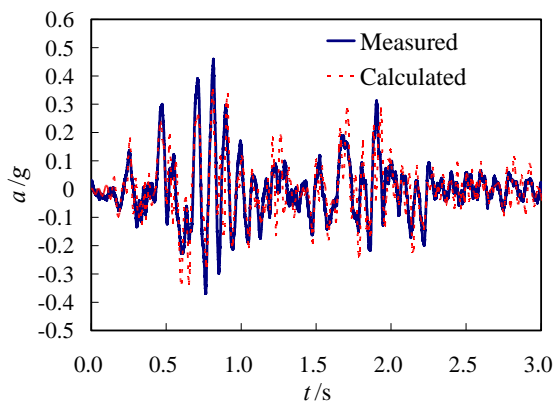Figure 8　Calculated and measured vibration mode

Figure 9 Acceleration time-history curve of the roof of SW subjected to earthquake excitation with peak ground acceleration of 0.231g (Before cracking)
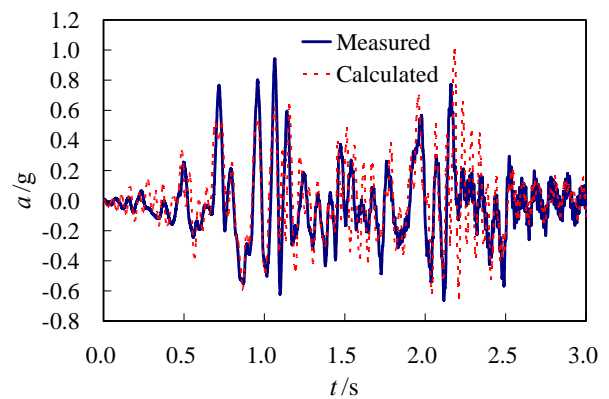

Figure 10 Acceleration time-history curve of the roof of SBW subjected to earthquake excitation with peak ground acceleration of 0.538g (Before cracking)

4.2 Nonlinear Time History Analysis

Nonlinear time history analyses are made using SAP for the two models at different stages. For the normal shear walls, the nonlinear parallel multi-component model was used in the bottom area of plastic hinge (Wang *et al*. 2002 and Jiang *et al*. 2003). For the shear walls with concealed bracings, the parallel and oblique multi-component model was used in the bottom area of the plastic hinge (Figure 11). The elastic elements were used in the areas where concrete cracks did not appear. The columns which support the shear walls is considered to be elastic for the reasons that the cracks are slender and appear later.

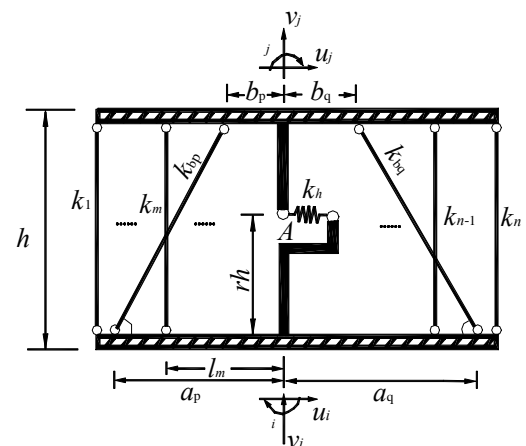Comparison at the failure stage of the nonlinear time

Figure 11 Element model of shear wall with concealed bracings

history analysis results and the measured results are shown in Figures 12 and 13. Figures 12 describes the acceleration history-time curve of SW after cracking. Figures 13 describes the acceleration history-time curve of SBW after cracking.
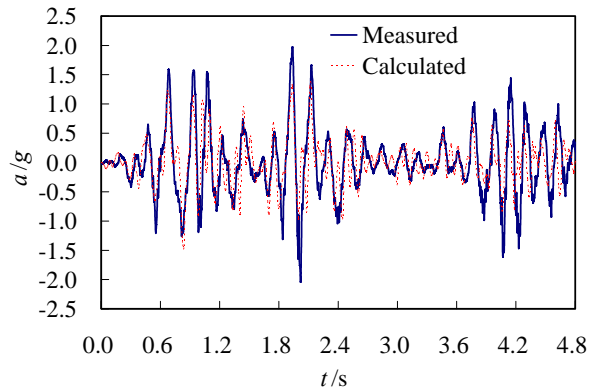

Figure 12 Acceleration time-history curve of the roof of SW subjected to earthquake excitation with peak ground acceleration of 1.17g (Failure stage)
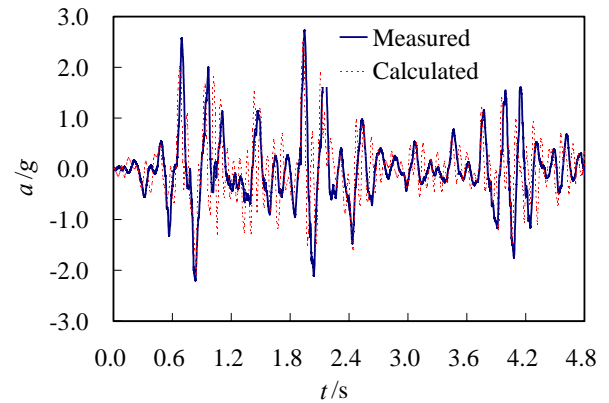
Figure 13 Acceleration history-time curve of the roof of SBW subjected to earthquake excitation with peak ground acceleration of 1.66g (Failure stage)

5 CONCLUSIONS

(1) At the elastic stage, the dynamical characteristics of the shear wall structure with concealed bracings and the normal shear wall structure without concealed bracings are almost the same. After concrete cracking, for the shear wall structure with concealed bracings, the attenuation of natural frequency is slower and the ground floor of the first vibration mode trends to develop less outward in comparison with the normal shear wall structure without concealed bracings.

(2) At the elastic stage, the acceleration response of the shear wall structure with concealed bracings and the normal shear wall structure without concealed bracings are almost the same. At the inelastic stage after the concrete cracking, the resistance of the shear wall structure with concealed bracings to seismic load is much better than that of the shear wall structure without concealed bracings. At the ultimate failure stage, the peak of the acceleration applied to excite the shear wall structure with concealed bracings is increased by 57.63% compared with that applied to excite normal shear wall structure without concealed bracings.

(3) For shear wall structures with and without concealed bracings and having large space on the ground floor, the interstory drift of the ground floor is significantly larger than that of the other three floors. At the elastic stage, the corresponding interstory drift responses of each floor for the two kinds of structure are similar. At the inelastic stage after the concrete cracking, the maximum value of the ground floor interstory drift response for the shear wall structure with concealed bracings is much less than that of the shear wall structure without concealed bracings.

(4) For the shear wall structure with concealed bracings, the maximum shearing force on the base, which is endured by the structure, is increased by 33.64% in comparison with that of the shear wall structure without concealed bracings.

(5) The failure modes of the shear wall with and without concealed bracings are different. For the normal shear

wall, there is only one main horizontal crack at the bottom of the wall. While for the shear wall with concealed bracings, there are main cracks respectively at the middle and the bottom of the wall, which indicates that the height of the plastic hinge areas at the bottom of the walls with concealed bracings are significantly larger than that of the normal walls without concealed bracings. This explains why the capacity of earthquake resistant and energy dissipation are improved.

ACKNOWLEDGEMENTS

REFERENCES

Cao, W.L. (1998) "A seismatic wall with concealed RC bracings, concealed half perforated crack and edge columns," *Patent Office of the People's Republic of China*, ZL 97244563.3.

Cao, W.L., Hu, G. Zh. and Pang, G. X. *et al*. (1999) "The mechanics calculation model of the aseismic walls with concealed bracings," *Earthquake Engineering and Engineering Vibration* (1), 212-218.

Dong, H.Y., Cui, L.C. and Cao, W.L., *et al*. (2001) "Influence of reinforcement proportion of the concealed bracings on seismic behavior of the R.C. shear wall," *Word Earthquake Engineering* 17(3), 73-79.

Dong, H.Y., Cao, W.L. and Huo, D. et al. (2002) "Nonlinear FEM analysis of R.C. short shear wall with concealed bracings," *Earthquake Engineering and Engineering Vibration* 22(5), 66-70.

Cao, W.L., Xue, S.D. and Zhang, J.W. (2003) "Seismic performance of RC shear wall with concealed bracing," *Advances in Structural Engineering* 6(1), 1-13.

Cao, W.L., Zhang, J.W. and Cui, L. Zh. et al. (2003) "Experimental study on seismic behavior of low-rise double-function R.C. shear wall with concealed bracings," *Journal of Building Structures* 24(1), 46-53.

JGJ3—2002 *Technical Regulations of High-Rise Building Concrete Structures*, China.

Li, J., Xiao, J. Zh. And Che, J. B. *et al*. (2002) "Earthquake Simulation Test on R.C. Special-Shaped Structure," *China Civil Engineering Journal* 35(3), 7-12.

Wang, M.F. and Zhou, X.Y. (2002) "The improved parallel multi-component model for the nonlinear seismic response analysis of R.C. walls and its application," *Journal of Building Structures* 23(1), 38-42.

Jiang, H.J. and Lü, X.L. (2003) "Research on application of macroscopic shear wall model," *Earthquake Engineering and Engineering Vibration* 23(1), 38-43.